Annealing processes in controlling the structures and properties of Solar Cell absorbed layer-$CuInSe_2$ films

XIN JI *, YIMING MI**, ZHI YAN[a], CHAO MIN ZHANG
College of Fundamental Studies, Shanghai University of Engineering Science, Shanghai 201620, China
[a]*College of Material Engineering, Shanghai University of Engineering Science, Shanghai 201620, China*

$CuInSe_2$ thin films were successfully deposited on SFO (SnO_2: F) glass substrates by magnetron RF-sputtering then annealed in vacuum at different temperatures (200, 250, 350 and 400 □). The effect of the annealing temperatures on the film structures, morphologies, and properties was investigated in detail. The results show that the CIS films with the room temperature by magnetron RF-sputtering was found to exhibit not amorphous but chalcopyrite phase structure. At the higher annealing temperatures the crystallinity and grain size were enhanced. Moreover, the 200 □ annealed CIS film shows better electrical behavior than other films. Finally, the optical measurements suggest that the optical property increased for annealing temperatures more than 200 □.

(Received August 3, 2011; accepted September 15, 2011)

Keywords: Thin film, $CuInSe_2$, Annealing processes, Vapor deposition, Optical properties

$CuInSe_2$ is one of the most promising materials for thin film solar cell applications, because it has a near optimal direct band gap. $CuInSe_2$ (CIS) is a semiconducting I-III-IV_2 compound with chalcopyrite structure. CIS films with a direct band energy gap of about 1.02 eV at 70 K for single crystal [1], which makes thin films with the thickness of only 1-2 μm, sufficient for the fabrication of the solar cells. In fact, conversion efficiencies close to 20% have already been achieved for evaporated $CuInSe_2$ based solar cells [2]. Thus, $CuInSe_2$ films are usually synthesized by various physical (PVD) and chemical vapor deposition (CVD) techniques such as: co-sputtering [3], flash evaporation [4-5], chemical spray [6] and electro-deposition [7]. These intensive investigations with alternative methods seek to obtain high-quality layer technologies. However, the full potential of these devices has not yet been realized for several reasons. Principal among these have been the difficulties in making stable low resistivity $CuInSe_2$ absorbed layer. In this result, various alternatives have been investigated. Many research efforts have been attempted to develop the prepared parameters with the ability to form a better property films [8-10]. It has been found that the structural, morphological and electro-optical properties of the material and the corresponding device performance are highly dependent on sputtering temperature and post-deposition treatments [11- 12].

Although the properties of the $CuInSe_2$ thin films are strongly dependent on prepared parameters in sputtering process, presently there is a lack of information in the literature regarding the systematic investigation on the relations between annealing temperatures and properties of the $CuInSe_2$ films. In this work, we focus on the transition of crystalline phase and improvement of the electrical and optical properties of $CuInSe_2$ films at various annealing processes. The acquired results and related discussions would be feasible for their potential applications.

1. Experiment

1.1 Synthesis of $CuInSe_2$ thin films

Thin films of CIS were deposited by RF-sputtering in argon gas atmosphere on SFO (SnO_2: F) glass substrates. Substrates were ultrasonically and chemically cleaned in organic solvents. A cylindrical $CuInSe_2$ (Cu: In: Se = 1:1:2) ceramic target of 8.0 cm diameter was used. No changes in target composition where observed with time and usage. Finally, films of CIS were annealed in vacuum at various temperatures (200, 250, 350 and 400 □). The process parameters of CIS films used in RF magnetron sputtering are shown in Table 1.

Table 1. Sputtering parameters of $CuInSe_2$ films.

Sample	Annealed temperature /(□)	Sputtering power / (W)	Sputtering temperature / (□)
a	25	100	25
b	200	100	25
c	250	100	25
d	350	100	25
e	400	100	25

1.2 Characterizations of $CuInSe_2$ films

Optical properties were determined from measurements of optical transmittance at room temperature with unpolarized light at normal incidence in the photon energy range of 1.1-6.6 eV. The resistivity calculated from the sheet resistance measured by a four-point probe. To investigate crystallographic properties of the films, coupled θ-2θ X-ray diffraction (XRD) scans in the film mode were performed in the range of $2\theta=20^o$-80^o by use of the Cu Kα1 line of the X-ray source (Rigaku D/max2550). The surface morphologies of films were examined by scanning electron microscopy (SEM-3400-N) and the surface roughness were examined by atomic force microscopy (AFM).

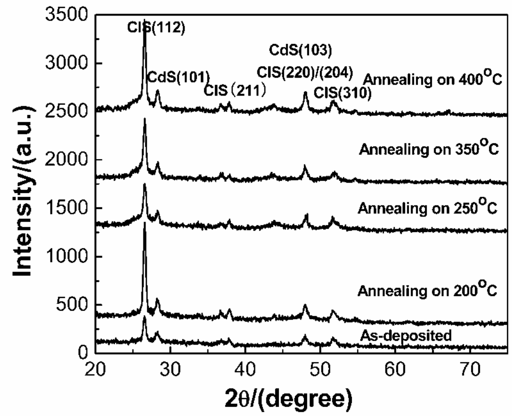

Fig. 1. XRD patterns of $CuInSe_2$ films prepared at various annealing temperatures.

2. Results and discussion

2.1 Structural studies of $CuInSe_2$ films

Fig. 1 shows the XRD patterns of $CuInSe_2$ thin films grown by magnetron RF-sputtering on SFO (SnO_2: F) substrates at room temperature. The film deposited at room temperature was found to be crystalline in nature as the film annealed at T = 200℃-400℃. Obviously, the room temperature XRD pattern by of CIS by magnetron RF-sputtering was found to exhibit not amorphous but chalcopyrite phase structure in contrast to the films in other methods such as electron beam deposition [13], because during synthesis, the sputtering pressure was kept at 0.5 Pa as a carrier gas which fully enhance the crystalline[14]. Moreover, the results show that the increase of annealing temperature is in favour to the diffusion of atoms absorbed on the substrate and accelerates the migration of atoms to the energy favorable positions, resulting in the enhancement of the crystallinity, and the three reflections (112), (211), (220) of the chalcopyrite structure[13] became apparent. In particular, the strong preferential orientation of the (112) plane was observed and the peak intensity was multiplied by about 30 times in comparison with the as-deposited films. The high peak intensity indicated that the crystallinity and/or grain size was enhanced by the annealing processes [15].

2.2 Morphological studies of $CuInSe_2$ films

The $CuInSe_2$ films have been analyzed by SEM techniques in order to observe and study the surface morphology of the films at various annealing temperatures. Fig. 2 shows the SEM micrographs with a scanning area of 3 μm in the CIS thin films. In the case of the films with as-deposited and annealed at 200 ℃ and a few isolated white grains (CdS grains) with uniform size and well-defined boundaries on the gray grains ($CuInSe_2$ grains) was observed, however, as the annealing temperature increased the CdS grains tend to agglomerate. In as-deposited CIS film, CdS grains are distributed over the surface of the $CuInSe_2$ grains, whereas only many rounded CIS grains have been observed in the annealed films. This is due to the diffusion of atoms was limited and thereby led to the CIS islands formatted on the substrate, which covered the CdS islands. Also, the improvement in crystallinity of the CIS grains occurred by the thermal energy acquired from the annealing treatment [13]. The films annealed at 200℃, 250℃ and 350℃ have a bigger CIS gain size than that of the as-deposited film. In addition, the grain size become much bigger when annealed at 400℃. This increase in the grains size is very important because it is reported [16, 17] that the efficiency in polycrystalline solar cells increases with increasing the grain size for the absorbing materials.

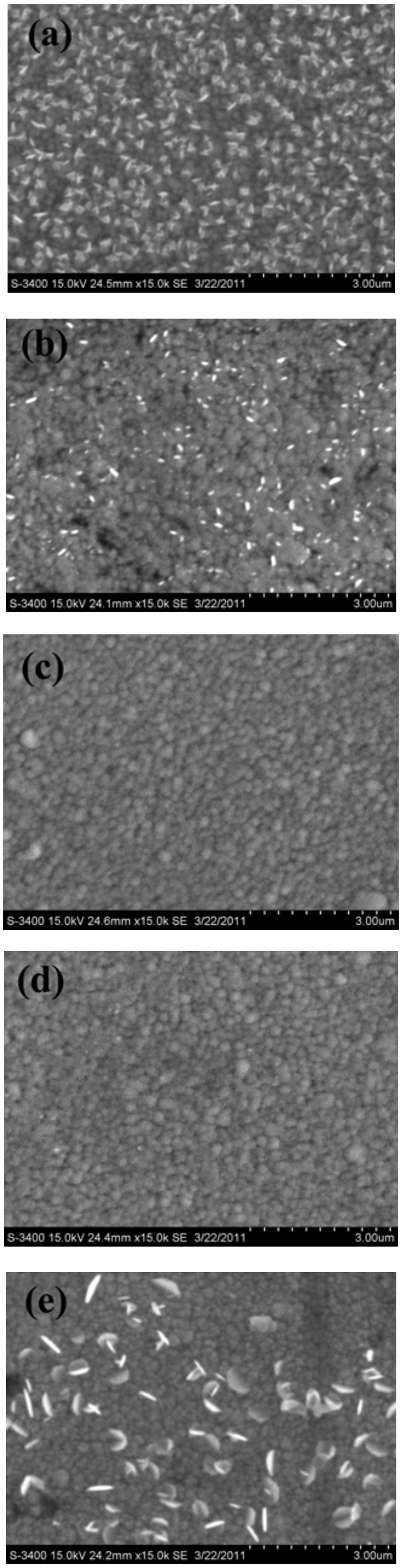

Fig. 2. SEM images of cross sections in $CuInSe_2$ films prepared at various annealing temperatures: (a) as-deposited; (b) 200 ℃; (c)250 ℃; (d)350 ℃; (e) 400 ℃

Table 2 summarizes the data of grain diameters and surface roughness in $CuInSe_2$ samples as resulted by AFM. It can be seen from Table 2 that the CIS films annealed at 250℃ and 400℃ displayed a rugged surface with a root mean square (RMS) roughness of about 11.408 and 12.175 nm, which might be related to the appearance of sub-grains. It was observed that the 350℃ annealed CIS film has a smoother surface than the other films. This result may be interpreted by S. Kuranouchi et al [15] that a phase separation of the surface layer occurred by annealing. These results indicated that the liquid (Cu, Se)-solid (CIS) growth mechanism was enhanced in the annealed films.

Table 2. Variation of grain diameters and surface roughness of CIS films prepared at different annealing temperatures.

Sample	Annealed temperature /(℃)	Grain diameter / (nm)	Surface Roughness /(nm)
a	25	66.526	9.800
b	200	80.718	9.826
c	250	82.661	11.408
d	350	73.858	9.568
e	400	124.231	12.175

2.3 Electrical properties of $CuInSe_2$ films

Fig. 3 illustrates the resistivity calculated from the sheet resistance measured by a four-point probe as a function of the annealing temperature for CIS films. It is observed from Fig. 3 that the electric conduction of CIS films decrease firstly and then increase with annealing temperatures. The film of 200℃ shows the better electrical behavior than other films, which is due to the secondary phase of chalcopyrite structure observed in XRD. Moreover, the higher conduction of 200℃ annealed CIS film because of a smoother surface can be interpreted by A. M. Hermann et al [18]. It is reported that smoother films show not only reduced light trapping at the surface, but also lowers the number of interface states between the absorber layer and the window layer in the device.

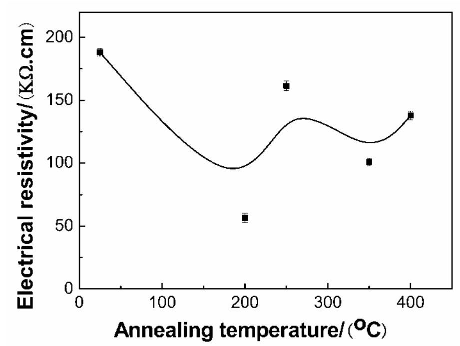

Fig. 3. The resistivity curves of $CuInSe_2$ films as a function of the annealing temperatures.

2.4 Optical properties of $CuInSe_2$ films

Fig. 4 shows the transmittance spectra curves of the CIS films annealed at various temperatures in the wavelength range 200-1100 nm. It can be observed that a sharp decrease in the transmittance with the increase of the annealing temperatures. This behavior was consistent with the increase of the grain sizes increase absorption coefficient of the films by the high temperatures annealing processes [19]. Moreover, it also can be found that the optical transmission of the CIS film at the same annealing temperature was increased gradually in the range from 380 to 780 nm. This is attributed to the increase in free-carrier absorption in the visible light wave due to the low electron mobility of the solar cell [20].

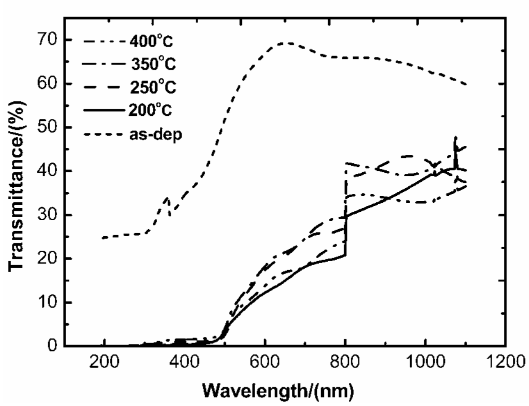

Fig. 4. Transmittance spectra curves of $CuInSe_2$ films prepared with various annealing temperatures.

3. Conclusions

1) The XRD patterns reveal that the film deposited at room temperature was found to be crystalline in nature as the film annealed. It suggests that vacuum annealing process at low temperature (not exceed to 400□) can result in the enhancement of the crystallinity of the CIS grains.

2) The result of SEM morphologies indicated that the grain size of CIS films and the efficiency in polycrystalline solar cells increases in the annealing processes.

3) The resistivity curves observe that the electric conduction of CIS films decrease firstly and then increase with the increase of annealing temperatures. The 200□ annealed CIS film shows better electrical behavior than other films.

4) The optical measurements suggest that the optical property of film increased for annealing temperatures more than 200□. It is concluded that not only the grain sizes but also the electron mobility in the annealing processes affected the optical properties of CIS films.

Acknowledgements

This work is supported by the Shanghai Municipal Education Commission's Fund for the Outstanding Young Teachers in High Education Institutions (No: gjd110033) and the Academic Program of Shanghai Municipal Education Commission (No: A-3500-11-10).

References

[1] M. G. Faraj, K. Ibrahim, A. Salhin, Optoelectron. Adv. Mater. – Rapid Commun. **4**(12), 2092 (2010).
[2] M. A. Popescu, J. Non-Cryst. Solids. **192/193**, 140 (1995).
[3] J. A. Thornton, T. C. Lommasson, H. Talieh, B. H. Tseng, Solar Cells. **1**, 24 (1988).
[4] D. Sridevi, K. V. Reddy, Indian J, Pure Appl. Phys. **24**, 392 (1986).
[5] H. Sakata, N. Nakao, Phys. Stat. Sol. A. **161**, 379 (1997).
[6] Y. D. Tembhurkar, J. P. Hirde, Thin Solid Films. **215**, 65 (1992).
[7] C. GuilleHn, J. Herrero, J. Appl. Phys. **71**, 5479 (1992).
[8] M. A. Popescu, J. Non-Cryst. Solids. **56**, 273 (1983).
[9] F. Chowdhury, J. Begum, M. S. Alam, S. M. F. Hasan, Optoelectron. Adv. Mater.-Rapid Commun. **4**(12), 2039 (2010).
[10] G. Z. Jia, Y. F. Wang, J. H. Yao, Optoelectron. Adv. Mater. – Rapid Commun. **4**(12), 2080 (2010).
[11] M. Chandramohan, T. Venkatachalam, Optoelectron. Adv. Mater.-Rapid Commun. **4**(1), 70 (2010).
[12] M. Ahmetoglu, Optoelectron. Adv. Mater. – Rapid Commun. **4**(4), 441 (2010).
[13] M. Venkatachalam, M. D. Kannan, S. Jayakumar, R.

Balasundaraprabhu, N Muthukumarasamy, Thin Solid Films, **20**, 516 (2008).
[14] T. Wada, N. Kohara, S. Nishiwaki, T. Negami, Thin Solid Films. **387**, 118 (2001).
[15] S. Kuranouchi, A. Yoshida, Thin Solid Film. **343/344**, 123 (1999).
[16] R. P. Singh, S. L .Singh, S. Chandra. J. Phys. D. **19**, 1299 (1986).
[17] U. Rau, M. Schmidt, A. J. Asenek, G. Hanna, H. W. Schock. Sol. Energy Mater. Sol. Cells. 67 (2001).
[18] A. M. Hermann, M. Mansour, V. Badri, B. Pink hasov, C. Gonzales, F. Fickett, M. E. Calixto, P. J. Sebastian, C. H. Marshall, T. J. Gillespie, Thin Solid Films. **74**, 361 (2000).
[19] I. Dirnstorfera, W. Burkhardt, W. Kriegseis, I. Osterreicher, H. Alves, D. M. Hofmann, O. Ka, A. Polity, B. K. Meyer, D. Braunger. Thin Solid Films. **361/362**,400 (2000),
[20] S. Shimakawa, Y. Hashimoto, S. Hayashi, T. Satoh, T. Negami, Sol. Energy Mater. Sol. Cells. **92**, 1086 (2008).

*Corresponding author: jixinyouxiang1@yahoo.com.cn
**yimingmi@sues.edu.cn